Cardiovascular Dynamics

Charles A. Taylor (1), Mary T. Draney-Blomme (1), C. Alberto Figueroa (1), Mary K. O'Connell (2), Peter Feenstra (1), Chengpei Xu (3), Christopher K. Zarins (3)

Departments of [1]Bioengineering, [2]Mechanical Engineering, [3]Surgery, Stanford University

INTRODUCTION

BACKGROUND

- Biomechanical factors important in maintaining normal vessel structure but can also impact congenital (coarctation) and acquired (atherosclerotic, hypertensive, aneurysmal) diseases.

OBJECTIVES

- Utilize 4D MRI analysis methods to characterize hemodynamic conditions and wall motion of the porcine and human thoracic and abdominal aorta.
- Construct a virtual aorta.
  - Create a 3D microstructural computational model of the medial lamellar unit (MLU), the building block of large blood vessels, using image-based modeling methods applied to confocal microscopy and serial block face scanning electron microscopy data.
  - Develop and apply homogenization methods to obtain equivalent macroscale properties for image-based microarchitectural model.
- Model blood flow and vessel wall deformation in normal subjects and patients with congenital and acquired diseases of the aorta.

RESULTS

QUANTIFICATION OF WALL MOTION USING 4D MRI

BACKGROUND:

- Mechanical environment of the thoracic aorta is largely unknown
- Designing and improved testing of new thoracic stent grafts

OBJECTIVE:

- Describe time- and location-dependent mechanics of the normal "young" and "mature" thoracic aorta

METHODS:

- 19 volunteers without history of cardiovascular disease were recruited and scanned according to a protocol approved by the Stanford University Institutional Review Board. Subjects were recruited into either a "younger" or "older" age group, which were defined as 20-35 years and 50-70 years, respectively. Young: n = 10; Mature: n = 9 (gender balanced).
- Contrast-enhanced MR angiogram obtained
- 4D volume of aortic motion (cardiac and respiratory resolved)
- ~12 aortic motion slices perpendicular to aorta

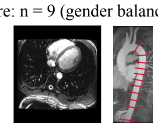

RESULTS:

- The distal thoracic aorta was found to have a smaller diameter but higher circumferential strain than the proximal aorta, and the direction of wall motion gradually rotated from the outer curvature in the proximal descending thoracic aorta to the inner curvature at the level of the celiac artery.

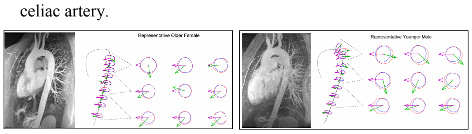

Figure 1. Aortic wall motion for representative older female subject and younger male subjects. For each panel - Left: Maximum intensity image from the MRA. Middle: Aorta centerline path and 3D luminal boundaries at time points of minimum (blue curve) and maximum (red curve) equivalent diameters. The magenta vectors point toward the inner curvature of the thoracic aorta, and the green vectors point in the primary motion direction. Right: The same luminal boundaries shown in 2D, rotated such the direction of the inner curvature is pointing to the left. All curves are shown to scale, with the magenta arrows at a fixed length of 20 mm.

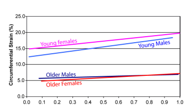

Figure 2. Circumferential strain down the length of the aorta for younger and older normal subjects.

WORK IN PROGRESS:

- Developing improved techniques for quantifying vessel wall motion.
- Quantify aortic wall motion in subjects with congenital and acquired vascular diseases.

3D NANOSTRUCTURE OF MEDIAL LAMELLAR UNIT

- Serial block-face scanning electron microscopy [Denk, 2006] used to create 3D images of the healthy rat aortic nanostructure
- Nanostructural data provides information on the complex 3D architecture & relationship of constituents within the medial lamellar unit (MLU), and serves as direct input into 3D microstructural computational model of the MLU
- Proportions of constituents:
  - Elastin = 30±6%, Cells = 29±18%
- Volume of Single Cell = 2024±428μm^3
  - Volume of Nucleus = 345±73μm3
  - Volume of Cytoplasm = 1680±355μm3
- Ellipticity of SMC nuclei = 6.2±1.5
- Radial tilt of SMC nuclei approximately 30°

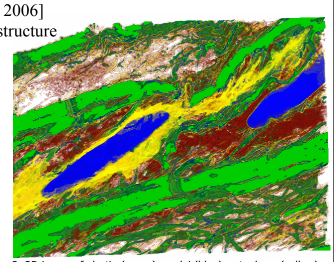

Figure 3: 3D image of elastin (green), nuclei (blue), cytoplasm (yellow), & collagen (red), showing extensive cytoplasm & radial tilt of nuclei

RESULTS

3D NANOSTRUCTURE OF MEDIAL LAMELLAR UNIT

Nanostructure Findings in Healthy Rat Aorta

- Elastin
  - Significant portion of elastin volume exists beyond lamellar boundaries
  - Thick struts connect adjacent lamellae
  - IEFs branching from lamellae form an extensive network
  - Thin IEFs extend obliquely to cell cytoplasm
- Cytoplasm
  - Cytoplasm fills in voids within interlamellar space
  - Cytoplasm extends toward and abuts IEFs and neighboring SMCs
  - Cytoplasm surface extends far beyond the nucleus & is highly irregular in shape

Figure 4: 3d image of elastin (brown) & nuclei (orange), showing thickness of strut connecting adjacent lamellae

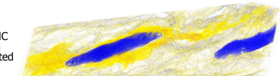

Figure 5: 3D image of SMC nuclei (blue) & cytoplasm (yellow), showing elongated nuclei with radial tilt and extensive cytoplasm

MODELING AORTIC BLOOD FLOW & AORTIC WALL MOTION

- Developed a new formulation to simulate blood flow in deformable subject-specific models
  - Computationally advantageous alternative to standard techniques for Fluid-Solid Interaction (FSI) phenomena
  - Enables representation of wall motion, wall stress & wave propagation phenomena in the cardiovascular system
  - Small increase in computational cost compared to rigid wall simulations

Strong Forms of the Navier-Stokes & Elastodynamics Equations

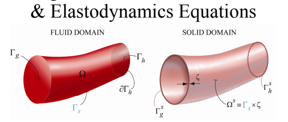

$\nabla\cdot\vec{v}=0$ $\rho\vec{v}_{,t}+\rho\vec{v}\cdot\nabla\vec{v}=-\nabla p+\nabla\cdot\underset{\sim}{\tau}+\vec{f}$	$(\vec{x},t)\in\Omega\times(0,T)$	$\rho^s\vec{u}_{,tt}=\nabla\cdot\underset{\sim}{\sigma}^s+\vec{b}^s$	$(\vec{x},t)\in\Omega^s\times(0,T)$
$\vec{v}=\vec{g}$ $\vec{t}_{\vec{n}}=\underset{\sim}{\sigma}\vec{n}=[-p\underset{\sim}{I}+\underset{\sim}{\tau}]\vec{n}=\vec{h}$ $\vec{t}_{\vec{n}}=\underset{\sim}{\sigma}\vec{n}=\vec{t}^f$	$(\vec{x},t)\in\Gamma_g\times(0,T)$ $(\vec{x},t)\in\Gamma_h\times(0,T)$ $(\vec{x},t)\in\Gamma_s\times(0,T)$	$\vec{u}=\vec{g}^s$ $\vec{t}_{\vec{n}}=\underset{\sim}{\sigma}^s\vec{n}=\vec{h}^s$	$(\vec{x},t)\in\Gamma_g^s\times(0,T)$ $(\vec{x},t)\in\Gamma_h^s\times(0,T)$
$\vec{v}(\vec{x},0)=\vec{v}^0(\vec{x});\quad p(\vec{x},0)=p^0(\vec{x})$	$\vec{x}\in\Omega$	$\vec{u}(\vec{x},0)=\vec{u}^0(\vec{x})$ $\vec{u}_{,t}(\vec{x},0)=\vec{u}_{,t}^0(\vec{x})$	$\vec{x}\in\Omega^s$

- Formulation Features:
  - Zero-velocity condition removed from the lateral surface of the fluid domain & replaced with a traction condition
  - Using a thin wall approximation, this unknown interface traction can be related to a body force, for the vessel wall (Womersley)
  - Traction of the fluid can be related through the elastodynamics equations with the mass and stiffness terms of the vessel wall
  - Membrane formulation used to describe mass and stiffness terms of the solid
  - Strong coupling approach is used whereby degrees-of-freedom of vessel wall & fluid boundary are same (i.e., no rotations) – solid momentum contributions are embedded into fluid equations using same degrees-of-freedom
  - Linearized kinematics approach adopted for coupled problem – enables representation of solid equations using the same Eulerian frame as in fluid equations
  - Linear membrane enhanced with transverse shear modes used due to lack of stability of linear membrane under transverse loading

$$
\begin{aligned}
B(\vec{w},q;\vec{v},p)=&\int_{\Omega}\left\{\vec{w}\cdot\left(\rho\vec{v}_{,t}+\rho\vec{v}\cdot\nabla\vec{v}-\vec{f}\right)+\nabla\vec{w}:\left(-p\underset{\sim}{I}+\underset{\sim}{\tau}\right)-\nabla q\cdot\vec{v}\right\}d\vec{x}\\
&-\int_{\Gamma_h}\vec{w}\cdot\vec{h}ds+\int_{\Gamma_h}qv_n ds\\
\boxed{\text{CMM-FSI terms}}\ &+\zeta\int_{\Gamma_s}\left\{\vec{w}\cdot\rho^s\vec{v}_{,t}+\nabla\vec{w}:\underset{\sim}{\sigma}^s(\vec{u})\right\}ds-\zeta\int_{\partial\Gamma_s}\vec{w}\cdot\vec{h}^s dl+\int_{\Gamma_s}qv_n ds\\
&+\int_{\Gamma_g}qv_n ds+\text{stabilization terms}=0
\end{aligned}
$$

Combined weak form for the Coupled-Momentum Method for Fluid-Solid Interaction (CMM-FSI):

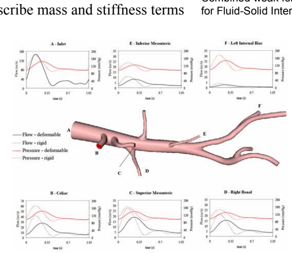

Figure 6. Pressure & flow waveforms obtained for rigid and deformable wall formulations using resistance BCs.

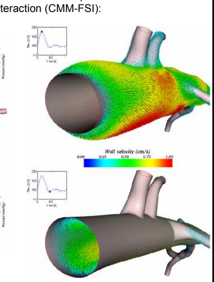

Figure 7. Vessel wall velocity vectors at two points of the cardiac cycle: peak systole (top) and early diastole (bottom)

- SUMMARY: Pressure waves show significantly larger pulses in the rigid case, whereas outflow waves present larger values in diastole and smaller values in peak systole for the deformable case.

DISCUSSION

IMPACT

- Image-based computational methods essential for quantifying biomechanical forces and elucidating structure-function relationships in blood vessels from nano- to macro-scales.
- Computational methods could be used to design novel therapies (pharmacologic, catheter-based, surgical) for aortic diseases.

FUTURE CHALLENGES

- Development of automated techniques for creating (i) time-varying image-based models from 4D MRI data, (ii) microstructural computational models from 3D microscopy data
- Development of nonlinear homogenization techniques to infer macroscale tissue properties from microscale data.
- Incorporation of external tissue support in coupled blood flow – vessel deformation simulations.

ACKNOWLEDGEMENTS

The authors would like to thank Winfried Denk and the Max Plank Society, Germany and NIH U54 GM072970. Volume Rover volume rendering software provided by UT Austin.